TIFR/BC/85-5
August, 1985

INCLUSIVE ϕ PRODUCTION IN K^-p INTERACTIONS AT 110 GeV/c AND SEARCH FOR STRUCTURE IN $\phi\pi^-$

(Bombay - CERN - Cracow - Innsbruck - London - Vienna - Warsaw Collaboration)

S.Banerjee, S.N.Ganguli, A.Gurtu, R.Raghavan, A.Subramanian
Tata Institute of Fundamental Research, Bombay, India

Y.Goldschmidt-Clermont, R.T.Ross*, S.Squarcia**
CERN, European Organisation for Nuclear Research, Geneva, Switzerland

K.Dziunikowska, T.Haupt
Institute of Nuclear Physics and Techniques, Academy of Mining and Metallurgy, Cracow and Institute of Nuclear Physics, Cracow, Poland

P.Girtler, D.Kuhn
Inst.für Experimentalphysik, Univ.Innsbruck, Innsbruck, Austria

K.W.J.Barnham, J.Wells***, P.R.S.Wright****
Blackett Laboratory, Imperial College, London, UK

J.Macnaughton, F.Mandl, F.Shabaan
Inst.für Hochenergiephysik, Oesterreich.Akad.Wissensch., Vienna, Austria

M.Bardadin-Otwinowska, M.Szczekowski
Institute of Experimental Physics, University of Warsaw and Institute for Nuclear Research, Warsaw, Poland

(Submitted to Z.Physik C)

* Now at Jet Joint Undertaking, Abingdon, UK
** Now at Physics Department, University of Genova, Itlay
*** Now at Department of Natural Philosophy, University of Glasgow, UK
**** Now at Nuclear Physics Laboratory, University of Oxford, UK

ABSTRACT

Results on inclusive ϕ production in K^-p interactions at 110 GeV/c are presented. The production cross section is found to be larger than in πp or pp interactions at similar energies, suggesting OZI allowed $s\bar{s}$ fusion to be the dominant mechanism in ϕ production. The x distributions of ϕ and $\bar{K}^{*0}$ are found to be similar to each other over the entire x range suggesting an overall strangeness suppression factor of 0.20 ± 0.04 in the sea to be the dominant source of the difference in the cross section for ϕ and $\bar{K}^{*0}$. There is no evidence of a narrow $\phi\pi^-$ state around 2.1 GeV/c^2 as suggested by K^+ experiments, but there is some excess of events in the region 1.94-1.98 GeV/c^2 consistent with the F-meson mass as observed in e^+e^- experiments.

1. INTRODUCTION

In this paper we investigate the inclusive production of ϕ mesons in K^-p interactions at 110 GeV/c. The study of inclusive meson resonances in soft hadronic collisions can give information on the constituent structure of fragmenting particles and on the dynamics of the interaction. In particular inclusive studies with kaon beams are of special interest since they may provide some insight on the structure function of the kaon.

The ϕ meson is the lightest member of a family of vector mesons with pure hidden quantum numbers [$\phi(s\bar{s})$, $J/\psi(c\bar{c})$, $\Upsilon(b\bar{b})$]. The ϕ is expected to be copiously produced in collisions of strange mesons with hadrons because of the strange valence quark in it unlike in πp or pp collisions. In K^-p interactions, there have been a few studies [1-4] at lower energies (10 GeV/c $\leq p_{lab} \leq$ 43 GeV/c). Only one experiment, that of the ACCMOR collaboration [5] has provided data at a comparable high energy of 63 and 93 GeV/c but only over a restricted x-region. There exists however more data on K^+p interactions [5-8], pp interactions [5, 9-13] and $\pi^{\pm}p$ interactions [1, 5, 11, 15].

The plan of the paper is as follows: the experimental details and the method of extracting ϕ signal are summarised in section 2. Section 3 contains experimental results on ϕ production. In section 4, we compare our results with a quark fusion model. In section 5, the results from a search of narrow resonances in $\phi\pi$ mode are given. Section 6 gives the summary and conclusion from the analysis.

2. EXPERIMENTAL METHOD

This analysis is based on a fully inclusive sample of 15K events corresponding to a sensitivity of 0.8 events/μb. The bias free sample was obtained from two exposures of the CERN bubble chamber BEBC to an r.f. separated, tagged K^- beam of 110 GeV/c nominal momentum. Details of the beam tagging, scanning, measurement of charged particles and of the data processing have been given in earlier publications [15-17].

The ϕ meson has been detected in the K^+K^- effective mass distribution. The invariant mass distribution has been obtained by assigning the kaon mass to all the charged secondaries excepting those for which the kaon hypothesis is excluded by ionisation estimates. A ϕ signal is seen in the K^+K^- mass spectrum for $x(K^+K^-) > 0.2$ (see dashed histogram in fig. 1a) where x is the Feynman x-variable. The ϕ signal to background ratio improves significantly as one restricts the sample to higher x-values (figs. 1b and 1c). However one expects a strong reflection of $\bar{K}^{*0}(890)$ into this mass spectrum. This will affect mostly the K^+K^- mass values higher than the ϕ mass region. If one investigates the $K^-\pi^+$ effective mass distribution (corresponding to a given K^-K^+ mass distribution by changing the mass of the positive track from kaon to pion) one finds a clear signal (not shown here; see ref.[17]) of $\bar{K}^{*0}(890)$.

2.1. Extraction of ϕ signal

In order to account for the $\bar{K}^{*0}(890)$ reflection, the $K^-\pi^+$ mass distributions are first fitted using

$$\frac{d\sigma}{dM_{\bar{K}\pi}} = BG_{\bar{K}\pi} \left[1 + \beta_{\bar{K}^*} BW_{\bar{K}^*}(M_{\bar{K}\pi}) \right] \qquad (1)$$

where $BW_{\bar{K}^*}$ is the relativistic P-wave Breit-Wigner given by

$$BW_{\bar{K}^*}(M_{\bar{K}\pi}) = \frac{M_{\bar{K}\pi}\, M_{\bar{K}^*}\, \Gamma(M_{\bar{K}\pi})}{(M^2_{\bar{K}\pi} - M^2_{\bar{K}^*})^2 + M^2_{\bar{K}^*}\, \Gamma^2(M_{\bar{K}\pi})} \qquad (2)$$

with

$$\Gamma(M_{\bar{K}\pi}) = \Gamma_{\bar{K}^*} \left(\frac{q_{\bar{K}\pi}}{q_{\bar{K}^*}}\right)^3 \frac{2q^2_{\bar{K}^*}}{q^2_{\bar{K}\pi} + q^2_{\bar{K}^*}} \qquad (3)$$

$M_{\bar{K}\pi}$ = effective mass of $K^-\pi^+$ system

$M_{\bar{K}^*}$, $\Gamma_{\bar{K}^*}$ = mass and width of $\bar{K}^{*o}(890)$

q_M = momentum of the decay product in the rest frame of invariant mass M

and the background term $BG_{\bar{K}\pi}$ is parametrised as

$$BG_{\bar{K}\pi} = a_1 \left(M_{\bar{K}\pi} - M_{\bar{K}} - M_\pi \right)^{a_2} \cdot \exp\left(-a_3 M_{\bar{K}\pi} - a_4 M^2_{\bar{K}\pi}\right) \qquad (4)$$

The resulting $K^-\pi^+$ mass distribution is fitted by fixing the $\bar{K}^*$ mass and width as given in the PDG table [18]. For each particle pair corresponding to an effective mass $M_{\bar{K}\pi}$ the probability that it does not originate from $\bar{K}^{*o}(890)$ can therefore be given by

$$W(M_{\bar{K}\pi}) = \frac{1}{1 + \beta_{\bar{K}^*} \cdot BW_{\bar{K}^*}(M_{\bar{K}\pi})} \qquad (5)$$

Each of the K^+K^- mass distributions can thus be corrected

for $\bar{K}^*$ reflection and the resulting distributions are shown by the solid histograms in fig. 1. These histograms are then fitted by a background term and a resonance term, the experimental resolution is folded in the latter;

$$\frac{d\sigma}{dM_{K\bar{K}}} = BG_{K\bar{K}} \left[1 + \beta_\phi \frac{\sqrt{2\pi}}{\delta} M_{K\bar{K}}\, \mathrm{Re}\{W(z_\phi)\}\right] \qquad (6)$$

where $\mathrm{Re}\{W(z_\phi)\}$ = real part of the complex error function,

$$z_\phi = \frac{M^2_{K\bar{K}} - M^2_\phi}{\delta\sqrt{2}} + i\,\frac{\Gamma_{K\bar{K}} \cdot M_\phi}{\delta\sqrt{2}}$$

δ = experimental resolution in $M^2_{K\bar{K}}$.

The value of δ is determined to be 0.03 GeV^2 from the data around the ϕ mass. For the background term $BG_{K\bar{K}}$ we use the parametrisation of the from (4) by replacing $M_{\bar{K}\pi}$ by $M_{K\bar{K}}$ and M_π by M_K. The width $\Gamma_{K\bar{K}}$ is parametrised as in eq. (3) by replacing the labels $\bar{K}\pi$ by $K\bar{K}$ and K^* by ϕ. The results of the fits are shown by the smooth solid curves in fig. 1. The contributions of background and resonance are shown by dash-dotted and dashed curves on the same figure. For $x > 0.2$, the number of ϕ's amount to 202 above the background.

In order to determine the differential distributions (in x and p_T^2) the ranges of these variables were first divided into suitable intervals and the effective K^+K^- mass spectra obtained for each of these intervals were then fitted in the way described above to extract ϕ signal.

3. RESULTS ON ϕ PRODUCTION

3.1. Inclusive ϕ Cross Section

The number of observed ϕ's has been corrected for unseen decay modes and the resulting ϕ cross section is 513 ± 80 μb for $x_\phi>0.2$ and 325 ± 44 μb for $x_\phi>0.4$, where x_ϕ is the Feynman variable. The error quoted here includes both statistical and systematic uncertainties due to background subtraction.

K^-p data at 10 and 16 GeV/c [1] give a cross section of 269 ± 50 μb for $x_\phi>0.2$. The data at 32 GeV/c [3] give total inclusive ϕ cross section as 700 ± 130 μb; if we assume that the x_ϕ distribution at 32GeV/c is the same as at 16GeV/c, we estimate the cross section at 32 GeV/c for $x_\phi>0.2$ to be ≈ 500 μb. In fig. 2 we have summarised the existing data of ϕ cross section in K^-p interactions [1,4] as well as K^+p [7,8] with $x_\phi>0.4$. From this one sees a slow increase in ϕ cross section with increase in beam momentum.

It should be noted that the ϕ cross section from pion and proton beams are significantly smaller. At 150 GeV/c π^+ and protons on a Be target [11] yield 148 ± 44 μb and 116 ± 26 μb respectively as ϕ cross section with $x_\phi>0.15$. Similar observations have been made by the ACCMOR collaboration [5] in a limited x_ϕ region by comparing ϕ production from $K^\pm$ with $\pi^\pm$, p and $\bar{p}$ at 63 GeV/c and 93 GeV/c.

3.2. Transverse momentum distribution

The transverse momentum distribution $d\sigma/dp_T^2$ for inclusive ϕ production with $x_\phi > 0.2$ is shown in figure 3. It is well described by a single exponential: $a\exp(-bp_T^2)$ with $a=(1110\pm270)\,\mu b/(GeV/c)^2$ and $b=(2.3\pm0.4)\,(GeV/c)^{-2}$. The value of the slope b can be compared with those obtained from 10-16 GeV/c (with no cut in x_ϕ) [1] and 43 GeV/c (with $x_\phi > 0.4$) [4] K^-p data which are 3.5 ± 0.3 and 3.3 ± 0.4 $(GeV/c)^{-2}$ respectively.

3.3. x-distribution (non-invariant)

The non-invariant $d\sigma/dx_\phi$ for inclusive ϕ production is given in table 1 and shown in figure 4. The x_ϕ- distribution can be fitted to the form $A_1(1-x_\phi)^{n_1}$ with $A_1=(1580\pm400)$ μb and $n_1=0.92\pm0.22$. For comparison, results of similar fits to the inclusive ϕ data at different beam energies and for different beams are summarised in table 2. From the table one can see that the ϕ meson spectrum is harder for $K^\pm$ beams than that for pion or proton beams. This suggests that the strange valence quark plays a dominant role in the production of ϕ in kaon beam.

We also show in figure 4 the non-invariant x distribution of $\bar{K}^{*o}$ in K^-p interactions at 110 GeV/c [17] for comparison with the present ϕ data. The shapes of ϕ and $\bar{K}^{*o}$ are remarkably similar over the entire x range. This is in agreement with the expectation of the additive quark model of Anisovich and Shekhter [19]; they also predict that in high energy K^-p interactions the production of ϕ meson is suppressed relative to $\bar{K}^{*o}(890)$ by a factor of λ which is the same in the central and fragmentation regions of the incident kaon. This factor measures the relative probability of extracting strange to nonstrange quarks from the sea. One obtains from 110 GeV/c K^-p data,

$$\lambda = \frac{\sigma(\phi\ ;\ x>0.2\ )}{\sigma(\bar{K}^{*o};\ x>0.2\ )} = \frac{513 \pm 80}{2580 \pm 210} = 0.20\pm0.04 \qquad (7)$$

This is to be compared with λ values of 0.12 ± 0.02 and 0.21 ± 0.05 obtained from the same reactions at 10 and 16 GeV/c K^-p [1] and 32 GeV/c K^-p [3] respectively. In a recent compilation of available data, Malhotra and Orava [20] have shown the strangeness suppression factor to be 0.27 ± 0.02 which is fairly independent of incident particles and c.m. energy (except a small threshold effect).

3.4. x-distribution (invariant)

The invariant x-distribution

$$F(x_\phi) = \int \frac{E}{\pi p_{max}} \cdot \frac{d^2\sigma}{dx\ dp_T^2} \cdot dp_T^2 \qquad (8)$$

has been evaluated and is shown in figure 5 (also given in table 1). The invariant x-distribution is rather flat as is indicated by a fit of the type

$$F(x_\phi) = A_2\ (1-x_\phi)^{n_2} \qquad (9)$$

with $A_2=(167\pm37)$ μb and $n_2=0.42\pm0.18$. For comparison similar values are tabulated in table 2 from other experiments. It is seen that the $F(x_\phi)$ distribution of the ϕ meson produced from $K^\pm$ beam is flatter than those from pion/proton beams. This may be expected because the ϕ contains a valence quark common with the beam particle for incident $K^\pm$, but not for other incident particles.

4. QUARK FUSION MODEL

In the quark fusion model [21,22] the invariant x-distribution can be written as the sum of three terms corresponding to OZI

allowed $s\bar{s}$ fusion and OZI suppressed $q\bar{q}$, $(q\neq s)$ and gg fusion, see fig.6. We give below the expression for $F(x_\phi)$ which incorporates the mass of the strange quark s (other partons u, d and g are assumed massless):

$$F(x_\phi) = \frac{4\pi}{3M_\phi^2}\left[\frac{g_A^2}{4\pi} \cdot J_s\{F_K^s(x_1).F_p^{\bar{s}}(x_2) + F_K^{\bar{s}}(x_1)\ F_p^s(x_2)\}+\right.$$

$$\frac{g_I^2}{4\pi} \cdot \sum_{\alpha=u,d} \{F_K^\alpha(x_1)\ F_p^{\bar{\alpha}}(x_2) + F_K^{\bar{\alpha}}(x_1)\ F_p^\alpha(x_2)\} +$$

$$\left.\frac{g_G^2}{4\pi} \cdot F_K^g(x_1)\ F_p^g(x_2)\right] \qquad (10)$$

where $J_s = (1-4m_s^2/M_\phi^2)^{-\frac{1}{2}}$. (11)

with m_s as the mass of the strange quark. The fractional longitudinal momenta x_1, x_2 $(0<x_{1,2}<1)$ of the colliding partons are given by,

$$x_1 = \frac{1}{2\sqrt{s}}\ (E_\phi + p_{\phi\parallel}) \cdot (1 + J_\alpha) \qquad (12)$$

$$x_2 = \frac{1}{2\sqrt{s}}\ (E_\phi - p_{\phi\parallel}) \cdot (1 + J_\alpha) \qquad (13)$$

where J_α for $s\bar{s}$ fusion is given by eq.(11) while for $q\bar{q}(q\neq s)$ and gg fusion $J_\alpha=1$. E_ϕ and $p_{\phi\parallel}$ are the energy and longitudinal momentum of ϕ in the c.m. system of energy $\sqrt{s}$. $F_{K,p}^i$'s are the structure funcions of the parton i in kaon and proton respectively.

$g_A^2/4\pi$, $g_I^2/4\pi$ and $g_G^2/4\pi$ are the coupling constants for $s\bar{s}$, $q\bar{q}$ and gg fusion respectively. Donachie et al [23] have estimated that the OZI suppressed coupling constant $g_I^2/4\pi$ is ≈6% of the OZI allowed coupling constant $g_A^2/4\pi$ by comparing $\phi \to 3\pi$ to $\omega \to 3\pi$ decay rates. In a recent analysis of ϕ production the ACCMOR group [5] has evaluated the three coupling constants and found that $g_I^2/4\pi$ and $g_G^2/4\pi$ are respectively 4% and 1% of the OZI allowed coupling $g_A^2/4\pi$. We have used the value of $g_A^2/4\pi=1.5$ as given in ref.[21], $g_I^2/4\pi$ and $g_G^2/4\pi$ to be 4% and 1% of $g_A^2/4\pi$ as obtained by [5].

For structure functions, we have used the parametrization as given in [25] for the proton and as in [24] for the kaon. These values are summarised in table 3. It is seen from the table that the structure function for the valence s quark in K^- is much flatter than the valence $\bar{u}$ quark because of the mass difference between the s and $\bar{u}$ quarks.

We have calculated the $F(x_\phi)$ distribution using eq. (10) for various values of m_s, the mass of the strange quark, in the range 0 to 0.4 GeV. The shape of the distribution does not change significantly for different values of m_s, but the overall cross section increases from 354 μb with m_s=0 to 552 μb with m_s=0.4 GeV for $x_\phi > 0.2$.

In order to fix the value of m_s we have made a simultaneous fit to the $F(x_\phi)$ distribution at 110 GeV/c, fig. 5, and the energy dependence of ϕ cross section with $x_\phi > 0.4$ shown in fig.2. This led to the estimate of m_s as 0.33 GeV and the solid curves in figs.2 and 5 show the fitted distributions. It is seen that the fitted curves reproduce the experimental data reasonably well. This may be regarded as a support, albeit indirect and model-dependent, for the assumed kaon structure functions.

5. SEARCH FOR STRUCTURE IN $\phi\pi$ INVARIANT MASS

In earlier experiments [26, 8] with K^+ beams at 32 and 70 GeV/c, some evidence was presented for a narrow resonance in $\phi\pi^+$ mass spectrum around 2.102-2.145 GeV/c^2. Anticipating that such state would be seen in $\phi\pi^-$ in our experiment we give the $\phi\pi^-$ invariant mass spectrum as a solid histogram in fig.7. The ϕ's have been selected using a cut on the mass $M(K^+K^-)$ between 1.01 and 1.05 GeV/c^2. Further cuts have been made on $x_\phi>0.2$ and $p_T(K^+K^-\pi^-)>0.8$ GeV/c, similar to those used in ref.[8, 26]. No evidence of any structure has been observed around 2.1 GeV/c^2 giving an upper limit (95% confidence level) of 10 μb for the signal at our energies. However the statistics and the mass resolution do not permit us to examine the mass distribution in intervals smaller than 40 MeV/c^2.

It may be noted from the fig.7 that there is some excess of events in the $\phi\pi^-$ plot in the mass range 1.94-1.98 GeV/c^2. This effect is not seen in the $\phi\pi^+$ mass spectrum which is shown as dashed histrogram in the figure. The statistical significance is rather meagre - the mass bin contains 15 combinations in $\phi\pi^-$ compared to 7 combinations in the $\phi\pi^+$ which is 1.5 standard deviation effect. This small excess is seen even after rebinning the histogram by shifting through half bin. A few e^+e^- experiments [27, 28] have claimed to observe the charm meson F decaying

to $\phi\pi^{\pm}$ in the same mass region. If the excess seen in fig. 7 is attributed to F^- production then the cross section times branching ratio for F production and decay within our experimental cuts amounts to 19±12 μb.

6. SUMMARY

We have presented the results from an inclusive study of ϕ meson production in K^-p interactions at 110 GeV/c. The inclusive cross section for $x > 0.2$ is 513±80 μb. A comparison with similar measurements in K^-p interactions at lower energies suggests a slow increase in ϕ cross section with increase in c.m. energy.

Comparison of inclusive ϕ and $\bar{K}^{*0}$ production in K^-p interactions at 110 GeV/c reveals the suppression of ϕ with respect to $\bar{K}^{*0}$ to be the same over the entire x-region explored. The strangeness suppression factor has been determined to be 0.20±0.04.

The non-invariant as well as the invariant x distributions of ϕ are rather flat which is in contrast to ϕ production data in pion or proton induced interactions. This suggests OZI allowed strange quark fusion to be the dominant mechanism in ϕ production.

Quark fusion model is able to reproduce the x distribution as well as the energy dependence of ϕ inclusive cross section.

There is no evidence of a narrow state in $\phi\pi^-$ mode around 2.1 GeV/c^2 as has been suggested by two earlier experiments with a K^+ beam at 32 GeV/c [26] and 70 GeV/c [8]. There is, however, some excess of events in the $\phi\pi^-$ mass region around 1.94-1.98 GeV/c^2 which is consistent with the F-meson mass seen in e^+e^- experiments [27,28].

ACKNOWLEDGEMENT

We are grateful to the BEBC staff for the successful operation of the bubble chamber and to the members of the EP division for their efficient work on the r.f.beam and the tagging system. The continuous support of the scanning and measuring staff at our laboratories is gratefully acknowedged.

REFERENCES

[1] P.Sixel et al., Nucl.Phys. B199, 381 (1982).

[2] C.Loudec et al., Nuovo Cim. 41A, 166 (1977).

[3] C.Cochet et al., Nucl.Phys. B155, 333 (1979)

[4] Yu M. Antipov et al., Sov.J.Nucl.Phys. 28, 670 (1978).

[5] C.Daum et al., Nucl.Phys. B186, 205 (1981); Z.Physik C18, 1 (1983)

[6] P.Garnet et al., Nucl.Phys. B140, 389 (1978).

[7] P.V. Chliapnikov et al., Nucl.Phys. B176, 303 (1980).

[8] M.Barth et al., Phys.Lett. 117B, 267 (1982).

[9] V.Blobel et al., Phys.Lett. 59B, 88 (1978).

[10] Yu.M.Antipov et al., Phys.Lett. 110B, 326 (1982).

[11] K.J.Anderson et al., Phys.Rev.Lett. 37, 799 (1976).

[12] D.Drijard et al., Z.Phys. C9, 293 (1981).

[13] J.G. Branson et al., Phys.Rev.Lett. 38, 1331 (1977).

[14] B.Ghidini et al., Phys.Lett. 68B, 186 (1977).

[15] G.Ransone et al., Nucl.Phys. B155, 307 (1979).

[16] G.Ransone et al., Nucl.Phys. B167, 285 (1980)

[17] R.Göttgens et al., Z.Phys. C12, 323 (1982).

[18] Review of Particle Properties, Phys.Lett. 111B (1982).

[19] V.V.Anisovich and V.M.Shekhter, Nucl.Phys. B65, 455 (1973).

[20] P.K.Malhotra and R.Orava, Z.Phys. C17, 85 (1983).

[21] R.Moore and A.Donochie, J.Phys. G4, 1885 (1978).

[22] A.Donachie and P.V.Landshoff, Z.Phys. C4, 231 (1980)

[23] A.Donachie and P.V.Landshoff, Nucl.Phys. B112, 233 (1976)

[24] P.V. Chliapnikov et al., Nucl.Phys. B148, 400 (1979).

[25] M.Gluck et al., Z.Phys. C13, 119 (1982).

[26] I.V.Ajienko et al., Phys.Lett. 35B, 451 (1980).

[27] A.Chen et al., Phys.Rev.Lett. 51, 634 (1983).

[28] M.Althoff et al., Phys.Lett. 136B, 130 (1984).

TABLE 1

Non-invariant and invariant ϕ production cross section in K^-p interactions at 110 GeV/c.

x_ϕ	$d\sigma/dx_\phi$ (μb)	$F(x_\phi)$ (μb)
0.2-0.4	942±343	99±36
0.4-0.6	927±176	150±28
0.6-0.8	524±111	118±25
0.8-1.0	175± 74	50±21

TABLE 2

Values of the exponents n_1 and n_2 from fits to x distributions of inclusive ϕ production.

Initial State	Beam Momenum (GeV/c)	n_1 in $d\sigma/dx_\phi \sim(1-x_\phi)^{n_1}$	n_2 in $F(x_\phi) \sim(1-x_\phi)^{n_2}$	Lower limit of x_ϕ used	Reference
K^-p	10 and 16	0.61±0.18	0.34±0.17	0.60	[1]
	43	0.98±0.13		0.40	[4]
	110	0.92±0.22	0.42±0.18	0.20	This work
K^+p	70	0.99±0.18		0.20	[8]
π^+p	16	1.8 ±0.3	1.05±0.41	0.00	[1]
π^+Be	150		1.73±0.44	0.15	[11]
π^+C	225		1.67±0.17	0.10	[13]
π^+Sn	225		2.16±0.24	0.10	[13]
π^-p	16	2.0 ±0.2		0.20	[14]
π^-C	225		1.60±0.24	0.10	[13]
p Be	70		6.0 ±1.7	0.41	[10]
	150		4.06±0.40	0.15	[11]
p C	225		3.82±0.14	0.10	[13]
p Sn	225		4.76±0.21	0.10	[13]

TABLE 3

Structure functions for kaon and proton.

K^-	Valence	$F_K^s = 2x(1-x)$; $F_K^{\bar{u}} = 0.85\ x^{0.5}\ (1-x)^{1.5}$
	Sea	$F_K^{u,\bar{u}} = F_K^{d,\bar{d}} = 2F_K^{s,\bar{s}} = 0.3(1-x)^5$
	Gluon	$F_K^g = 2(1-x)^3$
p	Valence	$F_p^u = 1.23\ x^{0.421}.(1-x)^{3.37}$; $F_p^d = 0.541\ x^{0.364}\ .\ (1-x)^{5.09}$
	Sea	$F_p^{u,\bar{u}} = F_p^{d,\bar{d}} = 4F_p^{s,\bar{s}} = 0.25\ (1-x)^7$
	Gluon	$F_p^g = 0.93\ (1+8.56x + 53.57x^2)\ (1-x)^6$

FIGURE CAPTION

1. K^+K^- mass distribution for (a) $x_{K^+K^-}>0.2$; (b) $x_{K^+K^-}>0.4$; (c) $x_{K^+K^-}>0.6$. The dashed histogram shows all the combinations and the solid histogram shows the combinations after subtraction of the $\bar{K}^{*0}$ reflection. The smooth solid curve is the results of the fit as described in the text. The dashed and dash-dotted curves are the contributions of the resonance and the background respectively.
2. Cross section for inclusive ϕ production with $x_\phi>0.4$ in K^-p and K^+p interactions as a function of beam momentum. The smooth curve refers to fusion model calcuation.
3. p_T^2 distribution of ϕ's produced in K^-p interactions with $x_\phi>0.2$. The line is a fit of the form $1.11\ \exp(-2.3p_T^2)$.
4. Feynman x distribution of inclusive ϕ production in K^-p interactions at 110 GeV/c. The open circles are for inclusive $\bar{K}^{*0}$ production [17]. The smooth curve is a fit of the form $1.58(1-x_\phi)^{0.92}$.
5. Invariant x distribution of inclusive ϕ (black circles) and $\bar{K}^{*0}$ [17] (open circles) in K^-p interactions at 110 GeV/c. The dashed curve is a fit of the form $0.167(1-x_\phi)^{0.42}$. The solid curve refers to fusion model calculation.
6. Parton diagrams for ϕ production : (a) OZI allowed strange quark fusion, (b) OZI inhibited non-strange quark fusion, (c) gluon fusion.
7. Effective mass distribution of $\phi\pi^-$ system with $x_\phi>0.2$ and $p_T(\phi\pi^-)>0.8$. The dashed histogram is the similar distribution for $\phi\pi^+$ system.

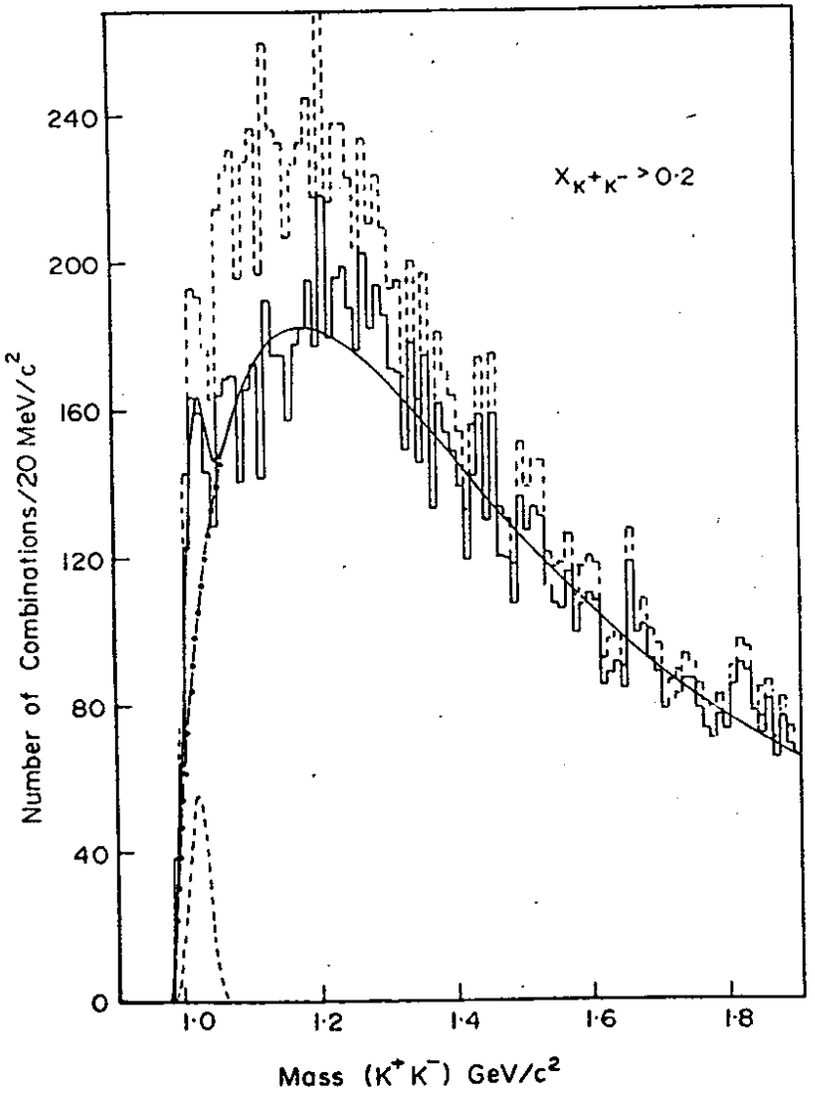
$X_{K^+K^-} > 0{\cdot}2$
Number of Combinations/20 MeV/c^2
Mass (K^+K^-) GeV/c^2
0
40
80
120
160
200
240
1·0
1·2
1·4
1·6
1·8

FIG. 1a

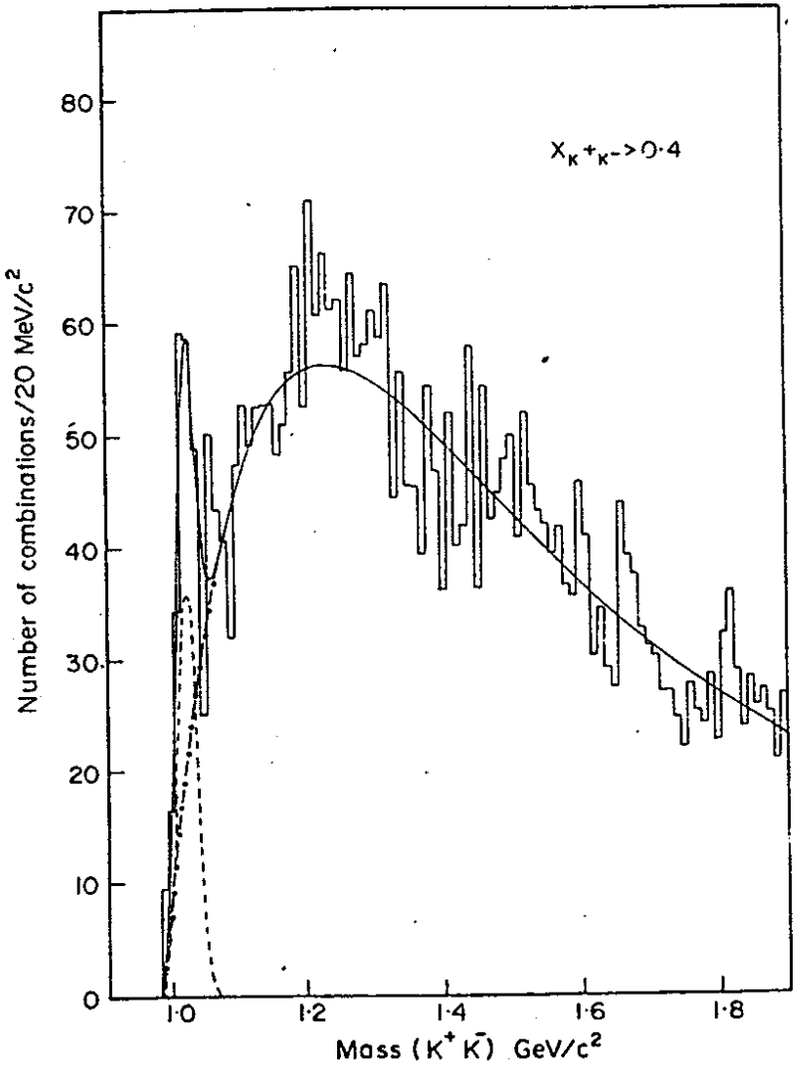
$X_{K^+K^-} > 0{\cdot}4$
Number of combinations/20 MeV/c^2
Mass ($K^+\bar{K}$) GeV/c^2
0
10
20
30
40
50
60
70
80
1·0
1·2
1·4
1·6
1·8

FIG. 1b

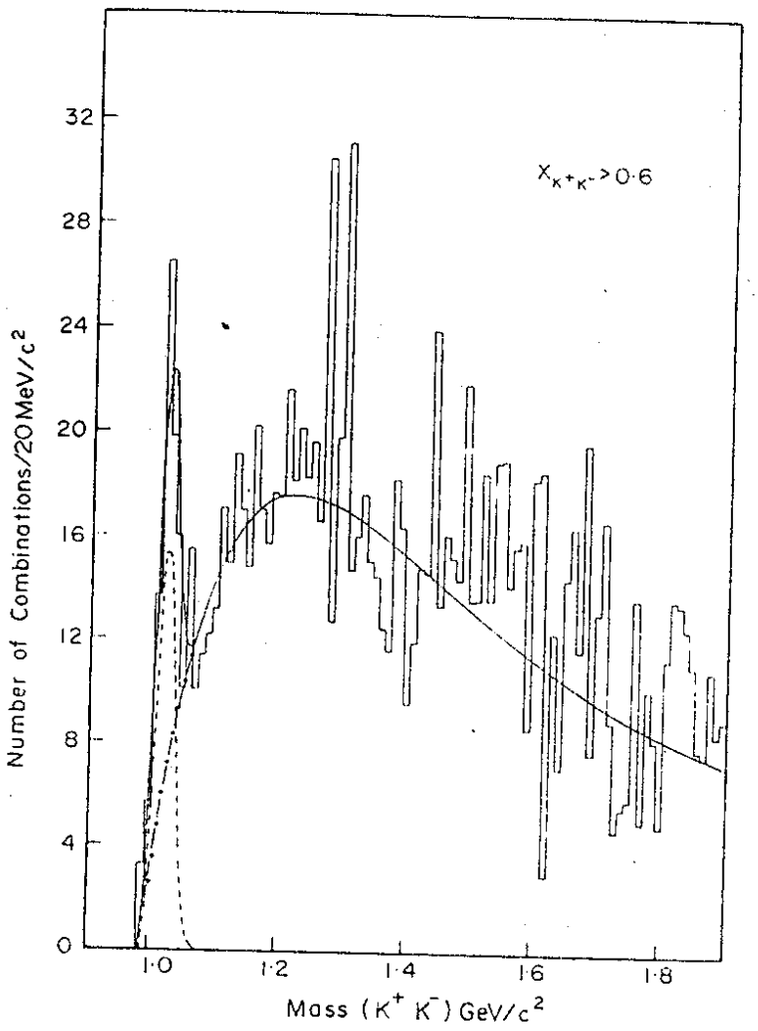
$X_{K^+K^-} > 0.6$
Number of Combinations/20 MeV/c²
Mass ($K^+ K^-$) GeV/c²
0
4
8
12
16
20
24
28
32
1·0
1·2
1·4
1·6
1·8

FIG. 1C

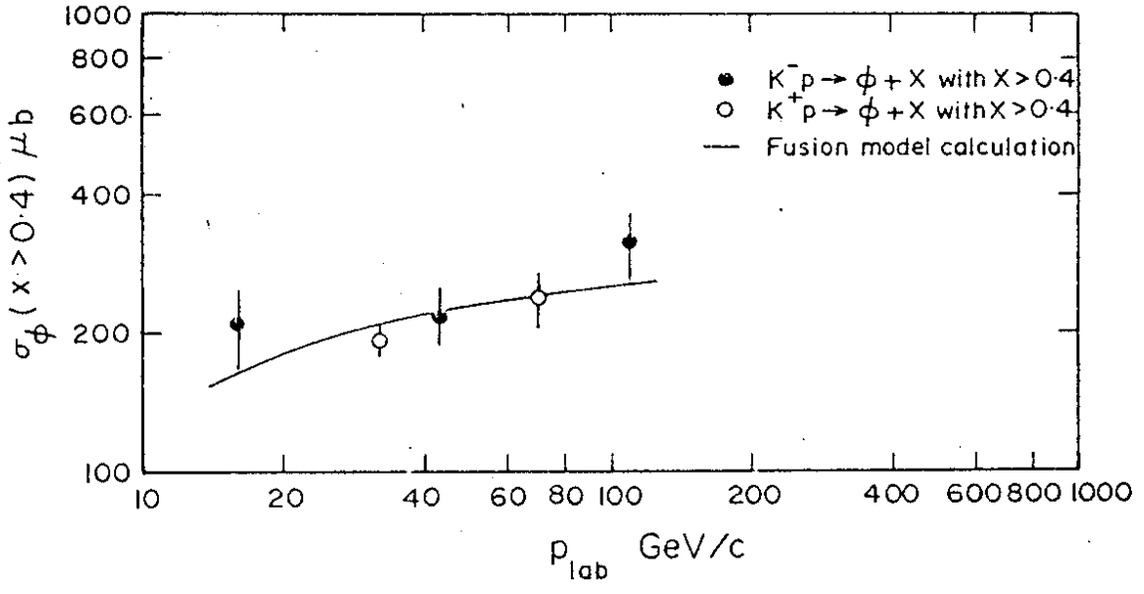
$K^- p \to \phi + X$ with $X > 0.4$
$K^+ p \to \phi + X$ with $X > 0.4$
Fusion model calculation
$\sigma_\phi (x > 0.4)\ \mu b$
p_{lab} GeV/c
100
200
400
600
800
1000
10
20
40
60
80
100
200
400
600
800
1000

FIG. 2

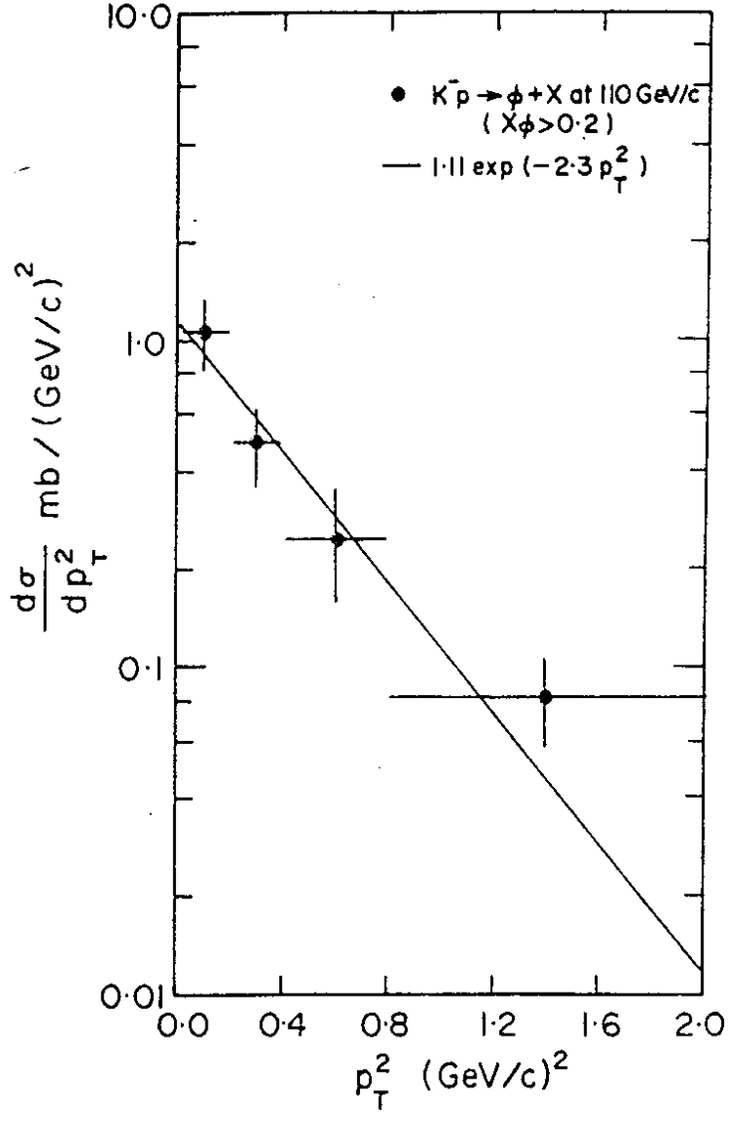
10·0
1·0
0·1
0·01
0·0
0·4
0·8
1·2
1·6
2·0
● K⁻p → φ+X at 110 GeV/c
(Xφ>0·2)
— 1·11 exp (−2·3 p_T²)
dσ/dp_T² mb / (GeV/c)²
p_T² (GeV/c)²

FIG. 3

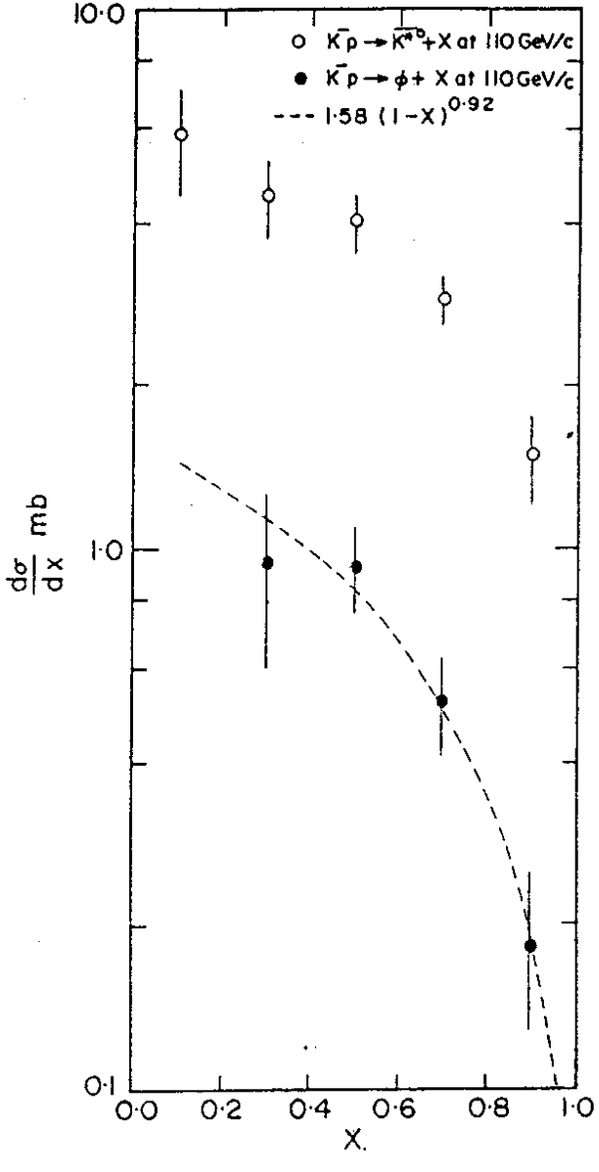
10·0
1·0
0·1
0·0
0·2
0·4
0·6
0·8
1·0
o K⁻p → K*⁰+X at 110 GeV/c
● K⁻p → φ+ X at 110 GeV/c
--- 1·58 (1−X)^0·92
dσ/dx mb
X.

FIG. 4

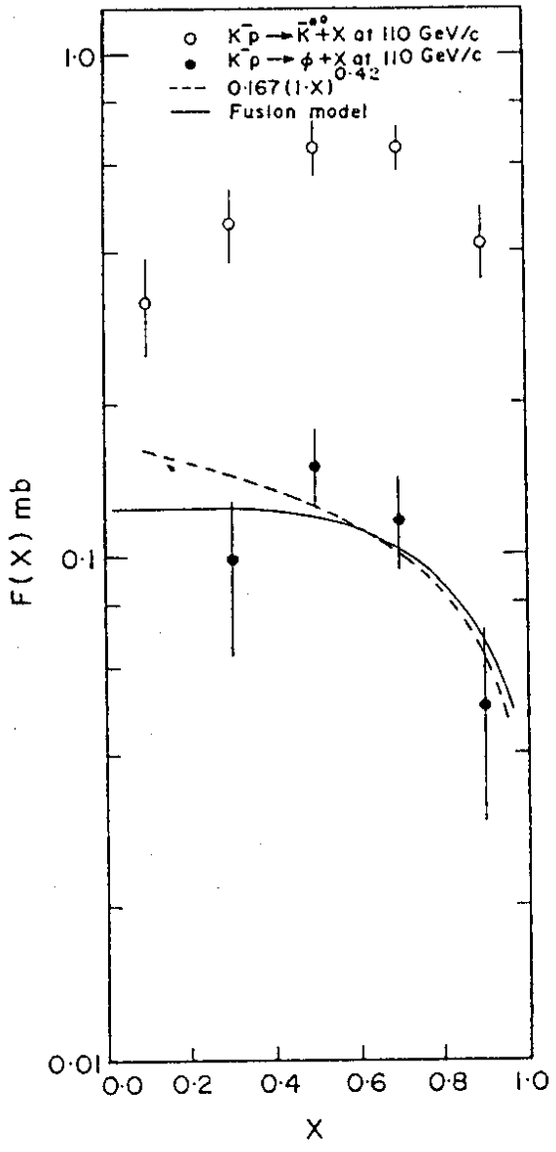

FIG. 5

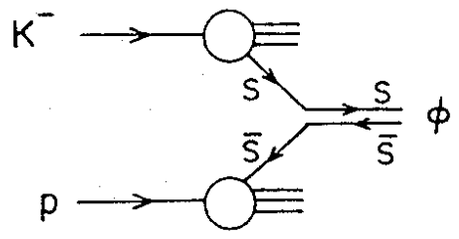

(a)

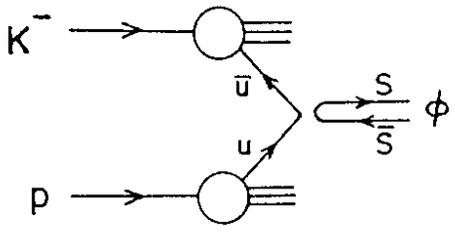

(b)

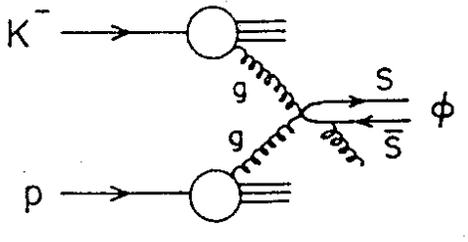

(c)

Fig. 6

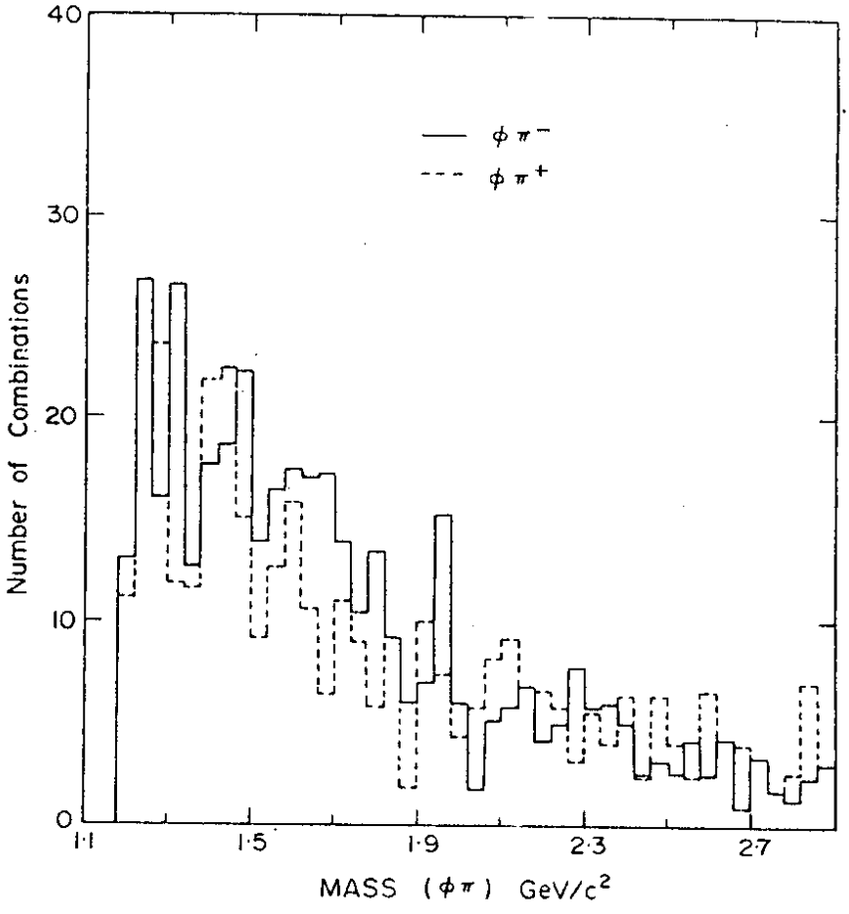
40
30
20
10
0
Number of Combinations
$\phi\pi^-$
$\phi\pi^+$
1·1
1·5
1·9
2·3
2·7
MASS ($\phi\pi$) GeV/c^2

FIG. 7